DMD Fast Forward. Published on December 9, 2009 as doi:10.1124/dmd.109.028712
This article has not been copyedited and formatted. The final version may differ from this version.

Title page

Glucuronidation of Dihydrotestosterone and Trans-androsterone by Recombinant UGT1A4: Evidence for Multiple UGT1A4 Aglycone Binding Sites

Jin Zhou

Timothy S. Tracy, PhD

Rory P. Remmel, PhD

Department of Medicinal Chemistry (J.Z. and R.P.R.) and Department of Experimental and Clinical Pharmacology (T.S.T.), University of Minnesota, Minneapolis, MN 55455, USA

Running title page

Running title: Atypical kinetics and multiple binding sites of UGT1A4

Address correspondence to Rory P. Remmel, Dept. of Medicinal Chemistry, College of Pharmacy, University of Minnesota, 308 Harvard St. SE, Minneapolis, MN 55455, Phone: 612-624-0472, e-mail: remme001@umn.edu

Text Pages: 30

Tables: 3

Figures: 8

References: 39

Abstract: 232 words

Introduction: 663 words

Discussion: 1480 words

Nonstandard abbreviations used in this paper: dihydrotestosterone (DHT); trans-androsterone (epiandrosterone) (t-AND); tamoxifen (TAM); lamotrigine (LTG); uridine-diphosphate glucuronic acid (UDPGA); Second-Order Akaike Information Criterion (AICc)

Abstract

UGT1A4-catalyzed glucuronidation is an important drug elimination pathway. Though atypical kinetic profiles (non-hyperbolic, non-Michaelis-Menten) of UGT1A4-catalyzed glucuronidation have been occasionally reported, systematic kinetic studies to explore the existence of multiple aglycone binding sites in UGT1A4 have not been conducted. To this end, two positional isomers dihydrotestosterone (DHT) and trans-androsterone (t-AND) were used as probe substrates and their glucuronidation kinetics with HEK293-expressed UGT1A4 were evaluated both alone and in the presence of a UGT1A4 substrate (tamoxifen (TAM) or lamotrigine (LTG)). Interestingly, co-incubation with TAM, a high affinity UGT1A4 substrate, resulted in concentration-dependent activation/ inhibition effect on DHT and t-AND glucuronidation, whereas LTG, a low affinity UGT1A4 substrate, non-competitively inhibited both processes. The glucuronidation kinetics of TAM were then evaluated both alone and in the presence of different concentrations of DHT or t-AND. TAM displayed substrate inhibition kinetics, suggesting that TAM may have two binding sites in UGT1A4. However, the substrate inhibition kinetic profile of TAM became more hyperbolic, as DHT or t-AND concentration was increased. Various two-site kinetic models adequately explained the interactions between TAM and DHT or TAM and t-AND. Also, the effect of TAM on LTG glucuronidation was evaluated. In contrast to the mixed effect of TAM on DHT and t-AND glucuronidation, TAM inhibited LTG glucuronidation. Our results suggest that multiple aglycone binding sites exist

within UGT1A4, which may result in atypical kinetics (both homotropic and heterotropic) in a substrate-dependent fashion.

Introduction

Glucuronidation, catalyzed by UDP glucuronosyltransferases (UGTs), is an important elimination pathway of various endogenous compounds such as steroid hormones, bile acids and bilirubin, as well as a large number of xenobiotics including drugs and their metabolites (Tukey and Strassburg, 2000). Of the 21 functional human UGT isoforms that have been characterized to date (Mackenzie et al., 2008), human UGT1A4 is often considered as the primary catalyst for N-glucuronidation due to its efficiency in catalyzing the glucuronidation of primary, secondary, tertiary and aromatic amines (Kiang et al., 2005). In addition to different amines, steroidal compounds with hydroxyl groups such as diosgenin and hecogenin are also UGT1A4 substrates (Green and Tephly, 1996).

Human UGTs are integral membrane proteins, with the majority of the protein, including the substrate binding sites (both aglycone and UDPGA), on the lumenal side of the endoplasmic reticulum membrane (Radominska-Pandya et al., 1999). Although an apo crystal structure of the cofactor UDPGA binding domain of human UGT2B7 has recently been published (Miley et al., 2007), the three-dimensional structures of the aglycone binding sites of UGTs are unknown and the interactions between their aglycone substrates and the substrate binding sites are poorly understood.

Similar to the cytochrome P450s such as CYP3A4, some UGT isoforms also exhibit atypical (non-Michaelis-Menten) kinetic features (Fisher et al., 2000; Uchaipichat et al., 2004; Iwuchukwu and Nagar, 2008; Ohno et al., 2008). Although the molecular mechanism(s) of atypical kinetics is still not fully established, numerous studies with the cytochrome P450s support the hypothesis that simultaneous binding of multiple molecules to the enzyme is involved (Shou et al., 1994; Korzekwa et al., 1998; Kenworthy et al., 2001; Shou et al., 2001; Galetin et al., 2002). Such detailed studies with UGTs are less prevalent. Recently Uchaipichat et al., examined 4-methylumbelliferone, 1-naphthol and zidovudine glucuronidation by UGT2B7. These authors concluded that the kinetic data provided evidence for the existence of multiple aglycone binding sites in UGT2B7 (Uchaipichat et al., 2008). Rios et al., also proposed that two or more aglycone binding sites may exist within UGT1A1, based on evaluations of the interactions of UGT1A1-catalyzed buprenorphine and bilirubin glucuronidation (Rios and Tephly, 2002).

Atypical kinetics of UGT1A4-catalyzed glucuronidation have also been reported (Chouinard et al., 2006; Hashizume et al., 2008; Hyland et al., 2009). However, systematic kinetic studies to explore the existence of multiple aglycone binding sites in UGT1A4 have never been conducted. Dihydrotestosterone (DHT) and trans-androsterone (t-AND) (Figure 1) are two steroidal substrates of UGT1A4. Although the glucuronidation of DHT and t-AND by UGT1A4 has been clearly established (Green and Tephly, 1996), a detailed kinetic analysis of these

processes has not been reported. These two compounds, based on a planar, rigid steroidal scaffold, differ only with respect to the position of the hydroxyl group (at position 3 or 17, the site of glucuronidation) and the location of the ketone group (position 17 or 3). Because of the rigid steroidal scaffold shared by these two compounds and the differing placement of substituents, these two compounds may either occupy the same region of the active site but in opposite orientation or occupy two separate regions in UGT1A4 active site. Studies in our lab on the activities of two polymorphic UGT1A4 enzymes (UGT1A4.2 and UGT1A4.3) demonstrated that mutations of amino acids in exon 1 of UGT1A4 exhibited a differential effect on DHT and t-AND glucuronidation (unpublished data). Because it is generally accepted that aglycone substrate binding sites of UGT1A enzymes are within the exon 1-coded N-terminal ends of the proteins (Radominska-Pandya et al., 1999), such polymorphism effects may indicate the possibility of DHT and t-AND occupying two separate regions in UGT1A4, reinforcing the need to conduct systematic kinetic studies with these two compounds to explore the existence of multiple aglycone binding sites in UGT1A4. To this end, a detailed characterization of the glucuronidation kinetics of these two compounds by HEK293-expressed UGT1A4 was conducted. Interactions of DHT or t-AND with another UGT1A4 substrate (tamoxifen (TAM) or lamotrigine (LTG), structures shown in Figure 1) were also evaluated.

Materials and Methods

Materials. Tamoxifen citrate and tamoxifen were purchased from MP Biomedical LLC (Santa Ana, CA). Lamotrigine was purchased from Toronto Research Chemicals Inc (North York, ON, Canada). Dihydrotestosterone, dihydrotestosterone glucuronide, trans-androsterone (epiandrosterone), tran-androsterone glucuronide and testosterone glucuronide were purchased from Steraloids, Inc. (Newport, RI). Lamotrigine N_2- glucuronide was a gift from GlaxoSmithKline (Philadelphia, PA). Uridine-diphosphate glucuronic acid (UDPGA), Trizma base, Trizma HCl, D-saccharic acid 1,4-lactone, alamethicin, morphine-3-glucuronide, and acetobromo-α-D-glucuronic acid methyl ester were purchased from Sigma-Aldrich (St. Louis, MO). $MgCl_2$ was purchased from Mallinckrodt Corp. (Hazelwood, MO). All other chemicals employed in the glucuronidation incubations, as well as the HPLC solvents were of HPLC grade. Chemicals used in the synthesis of tamoxifen –N-glucuronide were ACS grade. Recombinant UGT1A4 was produced in HEK293 cells (gift from Dr. Philip Lazarus, Penn State University, Hershey, PA). Cell lysate, prepared by sonication of UGT1A4-HEK293 cells in 10 mM Tris Buffer (pH=7.4 at 37˚C) containing 0.25 M sucrose for three 30-second bursts, each separated by 1-minute cooling on ice, was added directly to the incubation as the enzyme source. The protein concentration in cell lysate was determined with the Pierce BCA™ protein assay kit (Thermo Fisher Scientific Inc., Rockford, IL).

Synthesis of Tamoxifen-N- glucuronide (Kaku et al., 2004). Fifty mg (0.134 mmol) of Tamoxifen and 80.2 mg (0.202 mmol) of acetobromo-α-D-glucuronic acid methyl ester were dissolved in 0.4ml anhydrous dichloromethane and stirred for 72 hr at room temperature under nitrogen protection. The organic solvent was then removed by rotary evaporation. The resulting residue was dissolved in 3 ml of methanol and 1.5 ml of 0.5 M of aqueous sodium carbonate was added to the methanolic solution. The resulting solution was stirred at room temperature for five hrs. Twenty-five ml of water were then added to the reaction mixture, which was extracted five times with equal volumes of ether to remove unreacted tamoxifen. The pH of the aqueous layer was adjusted to 5.0 with 1 mol/l of HCl. Water in the aqueous layer was then removed by lypholization. The resulting residue was re-dissolved with a small volume of 0.1% formic acid in MeOH and loaded onto a preparative HPLC column (Higgins Haisil HL C18 5μm 100 x 20mm). The tamoxifen glucuronide was eluted with a mobile phase, consisting of 0.1% of formic acid in water-0.1% formic acid in MeOH (4:6 v/v), at a flow rate of 22 ml/min and monitored by UV absorbance at 254nm. The tamoxifen-N-glucuronide eluted at 16.5 min and collected fractions were pooled. Evaporation of the combined eluate fractions yielded 9.8 mg of white powder (13.2%). ^{1}H-NMR (600MHz, dimethyl sulfoxide-d6): δ 0.885 (t, 3H, *J* 7.2 Hz, CH_2CH_3), 2.409 (q, 2H, *J* 7.2 Hz, CH_2CH_3), 3.159-3.229(m, 7H, N-$(CH_3)_2$ and H-4′), 3.329 (m, 1H, H-3′), 3.464 (d, 1H, *J* 8.4 Hz, H-5′), 3.589 (m, 1H, H-2′), 3.843-3.886 (m, 2H, N-CH_2CH_2-O), 4.391 (m, 2H, N-CH_2CH_2-O), 4.694 (d, 1H, *J* 7.2 Hz, H-1′),6.716 (d,

2H, *J* 8.4 Hz, ArH, *ortho* to NCH_2CH_2O–), 6.80 (d, 2H, *J* 9 Hz, ArH, *meta* to NCH_2CH_2O–), 7.157–7.433 (m, 10H, ArH). ESI-TOF-MS: 548.2649$[M]^+$ (error 0.18ppm).

Incubations to Characterize Glucuronidation Kinetics in the Absence of Modifiers. Preliminary experiments were conducted to ensure that all kinetic determinations were carried out under linear conditions with respect to time and protein concentration. Incubation mixtures (200 µl final volume) contained UGT1A4-HEK293 cell lysate (0.25 mg/ml of protein for t-AND, DHT and LTG glucuronidation or 0.1mg/ml of protein for TAM glucuronidation), Tris-HCl buffer (0.1 M), $MgCl_2$ (5 mM), D-saccharic acid 1,4-lactone (5 mM), UDPGA (3 mM), alamethicin (50 µg/mg of protein) and DHT (3.9-250.0 µM), t-AND (2.8-202.2 µM), TAM (0.5-100 µM) or LTG (47.4-4969.8 µM). DHT, t-AND and TAM were initially dissolved in DMSO before addition to the incubation mixtures, whereas LTG was initially dissolved in 0.1 M acetic acid containing 4% of DMSO. The final organic solvent concentrations in all incubation mixtures were always less ≤2%. In each experiment, the organic concentration was constant irrespective of substrate concentration. The final pH of all incubation mixtures was 7.4 at 37˚C. Cell lysates were pre-incubated on ice with alamethicin for 30 minutes before reaction initiation. This step was followed by a 3-min preincubation at 37°C, after which the reaction was initiated by addition of UDPGA. After 30-min (DHT, t-AND and LTG) or 20-min (TAM) incubation in a shaking water bath, reactions were terminated by addition of 200 µl cold acetonitrile, followed by addition of internal

standards (DHT and t-AND glucuronidation assay: 20 µl of 1.07 µg/ml testosterone glucuronid; TAM glucuronidation assay: 10 µl of 14.2 µg/ml lamotrigine glucuronide; LTG glucuronidation assay: 10 µl of 50 µg/ml morphine-3-glucuronide). Protein precipitate was removed by centrifugation at 13,000 X g for 5 minutes and the reaction mixture was filtered through a 0.2 µ nylon spin filter (Grace Davison Discovery Science, Deerfield, IL) prior to injection onto the HPLC system.

Incubations to Characterize Interactions between UGT1A4 Substrates. The effect of TAM on DHT and t-AND glucuronidation was initially evaluated with three DHT or t-AND concentrations (approximately $0.5K_m$, K_m and $2K_m$) and six TAM concentrations (0, 1.25, 2.5, 5, 10, 20 µM). Because we observe a significant activation effect of TAM on DHT glucuronidation in this initial study, the effect of TAM on DHT glucuronidation was further evaluated with seven DHT concentrations (2.5-100 µM) in the absence or presence of five TAM concentrations (2.5-40 µM). The effect of LTG on DHT and t-AND glucuronidation was also evaluated with three DHT or t-AND concentrations (approximately $0.5K_m$, K_m and $2K_m$) and six LTG concentrations (0, 0.375, 0.75, 1.5, 3, 4.5 mM) and the effect of TAM on LTG glucuronidation was studied with three LTG concentrations (0.75, 1.5, 3 mM) and six TAM concentrations (0, 1.25, 2.5, 5, 10, 20 µM). The incubation conditions were as described above. In order to quantify dihydrotestosterone glucuronide by LC-MS, a liquid-liquid procedure was applied after reaction termination and protein precipitation. Fifty µl of 2.4

mol/l HCl solution were added to the incubation supernatants and the sample was extracted twice with 500 µl of ethyl acetate. The ethyl acetate extracts were then combined and dried under N_2 gas. Residues were reconstituted with 50 µl of water-acetonitrile (3:7 v/v) and 25 µl of the sample were injected onto the HPLC system for quantification. The recovery of the liquid-liquid extraction process was 100.2%±6.5% for dihydrotestosterone glucuronide and 96.9%±9.5% for internal standard testosterone glucuronide. To study the effect of DHT or t-AND on TAM glucuronidation, preliminary experiments were conducted at three concentrations of TAM (1.51, 7.57, 15.14 µM). Detailed kinetic studies on TAM (1.0-100 µM) glucuronidation were conducted in the presence of six DHT or t-AND concentrations (25 -250 µM). The incubation conditions were as previously described.

Chromatographic Analysis of Glucuronides. Two methods were developed to quantify trans-androsterone glucuronide and dihydrotestosterone glucuronide. To characterize the glucuronidation kinetics of DHT and t-AND in the absence of a modifier, trans-androsterone glucuronide and dihydrotestosterone glucuronide were quantified by an LC-MS/MS method with an Agilent 1100 series capilliary LC system coupled with a Thermo Finnigan TSQ quantum triple quadrupole mass spectrometer (Waltham, MA). Separation was carried out on a Thermo BetaBasic-18 column (150 x 0.5 mm, 3 µm, Waltham, MA). The mobile phase consisted of 10mM ammonium formate (A) and methanol (B) and was delivered at a flow rate of 12 µl/min. A linear gradient elution program, beginning with 50%

of mobile phase B, then increasing mobile phase B linearly from 50% to 90% over one minute and holding at 90% of B for 9 min was employed. The column was then re-equilibrated at initial conditions for 10 minutes. Both tran-androsterone glucuronide and dihydrotestosterone glucuronide eluted at 7.10 min and the internal standard testosterone glucuronide eluted at 6.71 min. The mass spectrometer was equipped with an ESI interface operated in negative ion mode. Quantification was accomplished in multiple reaction monitoring (MRM) mode by monitoring a transition pair of m/z 465→287 for trans-androsterone glucuronide and dihydrotestosterone glucuronide and 463→285 for the internal standard, testosterone glucuronide. Argon was used as the collision gas. The MS operating conditions were optimized as follows for transandrosterone glucuronide: spray voltage 4000V, sheath gas pressure 19mTorr, aux gas pressure 22mTorr, capillary temperature 355ºC, tube lens offset -95, collision pressure 2.2 mTorr, collision energy 46V; and as follows for dihydrotestosterone glucuronoide: spray voltage 3200V, sheath gas pressure 19mTorr, aux gas pressure 5mTorr, capillary temperature 355ºC, tube lens offset -95, collision pressure 1.9mTorr, collision energy 44V. When co-incubated with a modifier, trans-androsterone glucuronide and dihydrotestosterone glucuronide were quantified by a LC-MS method with a Shimadzu LCMS-2010A system (Columbia, MD). Chromatographic separation was accomplished on a Haisil column (C8, 100 x 2.1 mm, 5 µm, Higgins, Mountain View, CA). For quantitation of dihydrotestosterone glucuronide, the mobile phase consisted of 0.1% of formic

acid in water (A) and acetonitrile (B) delivered at a flow rate of 0.25 ml/min with a linear gradient elution program of: 30 to 67.5% of B over 5 min, followed by an isocratic hold at 95% of B for 5 min and a 4 min column re-equilibration at initial conditions. The retention times were for was 4.23 min for dihydrotestosterone glucuronide and 3.87 min for testosterone glucuronide. For the quantitation of trans-androsterone glucuronide, the same mobile phase was employed and a similar gradient elution program was applied: 30 to 60% B over 5 min, followed by an isocratic hold at 95% of B for another 5 min and a 4 min column re-equilibration at initial conditions. The retention times for trans-androsterone glucuronide and testosterone glucuronide were 3.60 and 3.23, respectively. The mass spectrometer was equipped with an ESI source operated in negative ion mode. Quantitation was accomplished in selected ion monitoring mode (SIM) by monitoring the respective $[M-H]^-$ ions: m/z=465 for trans-androsterone glucuronide and dihydrotestosterone glucuronide and m/z=463 for testosterone glucuronide. The MS parameters were as follows: nebulizing gas flow=1.5 L/min; interface bias = -3.50KV; interface current= -9.20 μA; heating block temperature= 200 °C; focus lens= +2.5V; entrances lens= 50.0V; RF gain= 5660; RF offset= 5210; prerod bias= +4.2V; main-rod bias= +3.5V; aperture= -20.0V; conversion dynode= +7.0kV; detector= -1.9KV; CDL voltage= -25.0kV; Q-array DC= -35.0 V; Q-array RF= +150.0V.

Both tamoxifen-N-glucuronide and lamotrigine-N_2-glucuronide were quantified by LC-MS methods (Shimadzu LCMS-2010A, Columbia, MD). Chromatographic

separation was accomplished on a Haisil column (C18, 100 x 2.1 mm, 5 μm, Higgins, Mountain View, CA). Mobile phase, 0.1% formic acid (A) and 0.1% formic in methanol (B) was delivered at a flow rate of 0.25 ml/min with the following linear gradient elution programs: for lamotrigine-N_2-glucuronide, 5% to 40% of B for 5 min, 40 to 80% of B for 3 min, an isocratic hold at 95% of B for 3 min, and column re-equilibration for 4 min (Lamotrigine glucuornide eluted at 6.92 min and the internal standard morphine-3-glucuronide at 2.90 min); for tamoxifen-N-glucuronide, 5 % to 40% of B for 5 min, 40 to 90% of B for 10 min, an isocratic hold at 95% of B for 3 min and, column re-equilibration for 4 min (Tamoxifen-N-glucuronide eluted at 15.68 min and internal standard lamotrigine glucuronide eluted at 5.96 min). The mass spectrometer was operated in positive ion mode with an ESI interface. Quantification was performed in single ion monitoring mode (SIM) by monitoring m/z=432 ($[M]^+$) for lamotrigine-N_2-glucuronide, m/z=548 ($[M]^+$) for tamoxifen-N-glucuronide and m/z=462 ($[M+H]^+$) for morphine-3-glucuronide. The MS parameters were set as follows: nebulizing gas flow=1.5 L/min; interface bias = +4.50KV; interface current= 11.60 μA; heating block temperature= 200 °C; focus lens= -2.5V; entrances lens= -50.0V; RF gain= 5620; RF offset= 5060; prerod bias= -4.2V; main-rod bias= -3.5V; aperture= +20.0V; conversion dynode= -8.0kV; detector= -1.5KV; CDL voltage= +25.0kV; Q-array DC= +35.0 V; Q-array RF= +150.0V.

Estimation of Non-specific Protein Binding. Free fractions of DHT, t-AND, TAM and LTG in incubation were estimated with the Hallifax-Houston model

DMD Fast Forward. Published on December 9, 2009 as DOI: 10.1124/dmd.109.028712
This article has not been copyedited and formatted. The final version may differ from this version.

(Equation 1)(Hallifax and Houston, 2006), where C is protein concentration in milligrams per milliliter and the logP values of DHT, t-AND , TAM and LTG are 3.428, 3.428, 6.064, 2.04 respectively and were calculated with Molinspiration-Interactive logP calculator (http://www.molinspiration.com/services/logp.html).

$$f_u = \frac{1}{1 + C \bullet 10^{0.072 \bullet \log P^2 + 0.067 \bullet \log P - 1.126}} \quad \text{(Equation 1)}$$

Data Analysis. Glucuronidation kinetic data for each substrate in the absence of modifiers were analyzed by fitting the Michaelis-Menten equation (Equation 2) or an empirical uncompetitive substrate inhibition equation (Equation 3) to the data with Sigma Plot 9.0 (Systat Software Inc., San Jose, CA) and by non-linear regression.

$$V_0 = \frac{V_{max} \times [S]}{K_m + [S]} \quad \text{(Equation 2)}$$

$$V_0 = \frac{V_{max}}{1 + \frac{K_m}{[S]} + \frac{[S]}{K_{si}}} \quad \text{(Equation 3)}$$

The V_{max} and K_m in Equation 2 were defined as the maximum velocity and substrate concentration at which velocity is equal to half of the maximum velocity. The V_{max} and K_m in Equation 3 have the same definition as in Equation 2 and K_{si} is the substrate inhibition constant. Selection of the appropriate model was determined by visual inspection of the Eadie-Hofstee plots and comparison of the Second-Order Akaike Information Criterion and the residual sum of squares.

DMD Fast Forward. Published on December 9, 2009 as DOI: 10.1124/dmd.109.028712
This article has not been copyedited and formatted. The final version may differ from this version.

Kinetic parameters were estimated by nonlinear regression analysis with Sigma Plot 9.0.

Glucurondation kinetics in the presence of modifiers were analyzed initially by calculating the percentage of rate of control (in the absence of modifiers). Modifiers that increased or decreased glucuronidation rate by greater than 20% were considered to exhibit activation or inhibition effects respectively. One-site competitive (Equation 4), noncompetitive (Equation 5), and mixed inhibition (Equation 6) models were applied to analyze the kinetic data, when only inhibition was observed. The V_{max} and K_m in Equation 4, 5, and 6 has the same definition as above. K_i is the inhibition constant. The parameter α reflects changes in the inhibition constant K_i. Selection of the appropriate model was determined by visual inspection of the Dixon plots and comparison of the Second-Order Akaike Information Criterion.

$$V_0 = \frac{V_{max} \times [S]}{K_m \times (1 + \frac{[I]}{K_i}) + [S]} \quad \text{(Equation 4)}$$

$$V_0 = \frac{V_{max} \times [S]}{K_m \times (1 + \frac{[I]}{K_i}) + [S] \times (1 + \frac{[I]}{K_i})} \quad \text{(Equation 5)}$$

$$V_0 = \frac{V_{max} \times [S]}{K_m \times (1 + \frac{[I]}{K_i}) + [S] \times (1 + \frac{[I]}{\alpha K_i})} \quad \text{(Equation 6)}$$

DMD Fast Forward. Published on December 9, 2009 as DOI: 10.1124/dmd.109.028712
This article has not been copyedited and formatted. The final version may differ from this version.

Various two-site kinetic models were applied to describe substrate inhibition kinetics as well as the interactions between TAM and DHT or TAM and t-AND (Figure 2 and Equation 7-11). Kinetic models with two-substrate binding sites have been successfully utilized to explain substrate inhibition kinetics (Houston and Kenworthy, 2000; Lin et al., 2001; Schrag and Wienkers, 2001). The two-site substrate inhibition model, incorporated herein, (Figure 2A, equation 7) assumes one reaction site and sequential binding of substrate molecules (Galetin et al., 2002). Kinetic models shown in Figure 2B (Equation 8) and Figure 2C (Equation 9) were used to describe the interactions between TAM and DHT. In these models, DHT (assumed to have one binding site in UGT1A4) interacts with the substrate inhibition site of TAM (assumed to have two binding sites in UGT1A4). Two kinetic models (Figure 2D and Equation 10; Figure 2E and Equation 11) were utilized to explain the effect of t-AND on TAM glucuronidation. These two models assume both t-AND and TAM have two binding sites in UGT1A4 and they compete for binding to UGT1A4 at both binding sites. In Figure 2D (Equation 10), the reaction site of t-AND overlaps with the reaction site of TAM. In Figure 2E (Equation 11), the reaction site of t-AND reaction overlaps with the substrate inhibition site of TAM. All the aforementioned two-site kinetic models assume rapid equilibrium (Segel, 1993). The kinetic parameter V_{max} equates to $k_p[E]_t$, where $[E]_t$ is the total enzyme concentration and k_p is effective catalytic rate constant . K_s, K_{DHT}, $K_{t\text{-}AND}$, K_{TAM} are binding affinity constants. Constants b and c reflect changes in k_p. Constant d reflects changes in binding affinity.

DMD Fast Forward. Published on December 9, 2009 as DOI: 10.1124/dmd.109.028712
This article has not been copyedited and formatted. The final version may differ from this version.

Surface plots were generated by fitting various two-site models to the kinetic data. Kinetic parameters were estimated with non-linear regression. Goodness of fit was determined by the residual sum of squares, Second-Order Akaike Information Criterion, standard errors of the parameter estimates and R^2.

$$V_0 = \frac{V_{max} \bullet (\frac{[S]}{Ks} + \frac{b \bullet [S]^2}{Ks^2})}{1 + \frac{[S]}{Ks} + \frac{[S]^2}{Ks^2}} \quad \text{(Equation 7)}$$

$$V_0 = \frac{V_{max} \bullet (\frac{[DHT]}{K_{DHT}} + \frac{c \bullet [TAM] \bullet [DHT]}{d \bullet K_{TAM} \bullet K_{DHT}})}{1 + \frac{[DHT]}{K_{DHT}} + \frac{[TAM]}{K_{TAM}} + \frac{[TAM]^2}{K_{TAM}^2} + \frac{[TAM] \bullet [DHT]}{d \bullet K_{TAM} \bullet K_{DHT}}} \text{(Equation 8)}$$

$$V_0 = \frac{V_{max} \bullet (\frac{[TAM]}{K_{TAM}} + \frac{b \bullet [TAM]^2}{K_{TAM}^2} + \frac{c \bullet [TAM] \bullet [DHT]}{d \bullet K_{TAM} \bullet K_{DHT}})}{1 + \frac{[DHT]}{K_{DHT}} + \frac{[TAM]}{K_{TAM}} + \frac{[TAM]^2}{K_{TAM}^2} + \frac{[TAM] \bullet [DHT]}{d \bullet K_{TAM} \bullet K_{DHT}}} \text{(Equation 9)}$$

$$V_0 = \frac{V_{max} \bullet (\frac{[TAM]}{K_{TAM}} + \frac{b \bullet [TAM]^2}{K_{TAM}^2} + \frac{c \bullet [TAM] \bullet [t-AND]}{d \bullet K_{TAM} \bullet K_{t-AND}})}{1 + \frac{[t-AND]}{K_{t-AND}} + \frac{[t-AND]^2}{K_{t-AND}^2} + \frac{[TAM]}{K_{TAM}} + \frac{[TAM]^2}{K_{TAM}^2} + \frac{2 \bullet [TAM] \bullet [DHT]}{d \bullet K_{TAM} \bullet K_{t-AND}}} \text{(Equation 10)}$$

$$V_0 = \frac{V_{max} \bullet (\frac{[TAM]}{K_{TAM}} + \frac{b \bullet [TAM]^2}{K_{TAM}^2} + \frac{c \bullet [TAM] \bullet [t-AND]}{d \bullet K_{TAM} \bullet K_{t-AND}})}{1 + \frac{[t-AND]}{K_{t-AND}} + \frac{[t-AND]^2}{K_{t-AND}^2} + \frac{[TAM]}{K_{TAM}} + \frac{[TAM]^2}{K_{TAM}^2} + \frac{[TAM] \bullet [DHT]}{d \bullet K_{TAM} \bullet K_{t-AND}}} \quad \text{(Equation 11)}$$

Results

Non-Specific Binding of DHT, t-AND, TAM and LTG. The estimated free fractions of DHT and t-AND were both 81.2% in incubations with 0.25 mg/ml of protein and 91.8% at a protein concentration of 0.1mg/ml of protein. The free fraction of LTG (0.25 mg/ml of protein) was estimated to be 95.2%, which is consistent with the negligible binding of LTG to HEK293 cell lysate reported by Rowland et al (Rowland et al., 2006). Since the estimated non-specific binding of DHT, t-AND and LTG under the incubation conditions employed was less than 20%, the concentration of DHT, t-AND and LTG added to the incubation mixtures was not corrected for non-specific protein binding in calculations of kinetic parameters. However, the estimated free fraction of TAM was 11.4% (0.1 mg/ml of protein) or 4.5% (0.25mg/ml of protein). TAM concentrations added to the incubation mixtures were corrected for binding when estimating kinetic parameters.

Kinetics of DHT and t-AND Glucuronidation. Initial efforts focused on conducting a detailed evaluation of the kinetics of DHT and t-AND glucuronidation. The Michaelis-Menten equation (Equation 2) was fit to the data for DHT glucuronidation whereas an empirical uncompetitive substrate inhibition equation (Equation 3) were fit to the data for t-AND glucuronidation. Results are presented in Figure 3 and the kinetic parameters obtained by non-linear regression are presented in Table 1. Though data for t-AND glucuronidation was not visually different from fits with the Michaelis-Menten equation in the Rate~[S]

plot , fitting the uncompetitive substrate inhibition equation to the data for t-AND glucuronidation generated a lower Second-Order Akaike Information Criterion (AICc) than fitting the Michaelis-Menten model to the data. (∆AICc was 19; a value for ∆AICc greater than 10 indicates essentially no support for the unfavorable model (Collom et al., 2008)). Also, Eadie-Hofstee plots of each dataset (Figure 3) clearly demonstrated differences between the kinetic profiles of DHT and t-AND glucuronidation. A two-site substrate inhibition model (Figure 2A, Equation 7) was also utilized to describe the data for t-AND glucuronidation. The estimated kinetic parameters with this model are presented in Table 2.

Effect of TAM on DHT and t-AND Glucuronidation. To test whether differential inhibition can be observed, DHT or t-AND, was co-incubated with a high affinity UGT1A4 substrate, TAM. TAM, a tertiary amine, forms a quaternary ammonium glucuronide upon UGT1A4-catalyzed N-glucuronidation. The reported K_m for TAM glucuronidation with recombinant UGT1A4 is 2.0 ± 0.51 μM (uncorrected for non-specific binding) (Sun et al., 2006), which was approximately 10-fold lower than the K_m values for glucuronidation of t-AND and DHT observed in the present study, suggesting that TAM may serve as a good competitive inhibitor. However, in contrast to the expected competitive inhibition, TAM caused concentration-dependent activation/ inhibition of both DHT and t-AND glucuronidation (Figure 4A and 4B). Notably, for DHT glucuronidation (Figure 4A), the maximum velocities occurred at concentrations below the highest TAM concentration; i.e. the velocities of DHT glucuronidation initially increased but

later decreased as TAM concentration was increased. In addition, the extent of activation effect increased as DHT concentration increased and the greatest activation was observed at the highest substrate concentration. Statistical comparison of DHT glucuronidation in the presence and absence of 10 μM TAM (uncorrected concentration) at 40 μM DHT indicated that the degree of activation by TAM was statistically significant (Student's t-test, $P<0.001$, $n=6$). With respect to t-AND glucuronidation (Figure 4B), the activation effect of TAM was less pronounced, but similar features as described above were noted (Figure 4B). The velocity of t-AND glucuronidation initially increased but later decreased with increasing TAM concentration and the extent of activation increased as t-AND concentration was increased.

To better understand the unexpected mixed effects of TAM on DHT glucuronidation, the Michaelis-Menten model (Equation 2)was fit to individual kinetic data sets. The obtained kinetic parameters are shown in Table 3. Both K_m and V_{max} of DHT glucuronidation increased as TAM concentration was increased. Also simultaneously fitting of all kinetic data with a proposed two-site model (Figure 2B and Equation 8) was conducted and is presented in Figure 5. Estimated kinetic parameters are presented in Table 2. In the two-site model (Figure 2B and Equation 8), DHT competes with TAM for binding to the substrate inhibition site of TAM. Models in which DHT competes with TAM for binding to the reaction site of TAM were also used to describe the kinetic data but much

larger standard errors of the parameter estimates and Second-Order Aikeike Information Criterion were obtained.

Kinetics of TAM Glucuronidation. Because of the unexpected effect of TAM on DHT and t-AND glucuronidation, the kinetics of TAM glucuronidation with recombinant UGT1A4 were evaluated. TAM glucuronidation exhibited substrate inhibition kinetics (Figure 6). Both the uncompetitive substrate inhibition model (Equation 3) and a two-site model (Equation 7) were fit to the kinetic data. The derived kinetic parameters are presented in Table 1 and 2 respectively. A constant free fraction of 11.4% for TAM was assumed in calculations of the kinetic parameters.

Effect of LTG on DHT and t-AND Glucuronidation. Another amine substrate of UGT1A4, LTG, was also evaluated as a modifier of DHT and t-AND glucuronidation. LTG also forms a quaternary ammonium glucuronide upon UGT1A4-catalyzed-N-glucuronidation. Initially, the kinetics of LTG glucuronidation were evaluated alone. LTG glucuronidation exhibited a hyperbolic kinetic profile (data not shown) with an estimated K_m of 1.6 ± 0.13 mM (Table 1). LTG at concentrations ranging from ~0.25 Km to ~3 Km inhibited DHT and t-AND glucuronidation (Figure 4C and 4D). Single-site competitive, noncompetitive and mixed inhibition models were evaluated to describe the inhibition data. The noncompetitive inhibition model was associated with the lowest AICc values in both cases. The model-predicted lines and observed data

are shown in Dixon plots (Figure 7A and 7B). The derived K_i were 3.25 ± 0.26 mM and 2.16 ± 0.24 mM for DHT and t-AND glucuronidation respectively.

Effects of TAM on LTG glucuronidation. To investigate whether TAM can activate UGT1A4 with substrates not based on the steroidal ring structure, we also studied the effect of TAM on LTG glucuronidation. At all TAM concentrations tested in the present study, LTG glucuronidation was inhibited (Figure 4E). A one-site competitive inhibition model was best fit to the inhibition data (Figure 7C). The K_i for this interaction was 0.31μM (TAM concentration was corrected for non-specific protein binding).

Effects of DHT and t-AND on TAM glucuronidation. Finally, the effects of DHT and t-AND on TAM glucuronidation were evaluated to assess whether the activation effects were bi-directional. Both t-AND and DHT inhibited TAM glucuronidation in a preliminary study (data not shown). To gain further insight into the interactions of DHT and t-AND on TAM glucuronidation, the kinetics of TAM glucuronidation were evaluated in the presence of six concentrations of DHT or t-AND. A two-site substrate inhibition model (Equation 7) was applied to fit the individual kinetic data sets. Although there were no clear trends of changes in the predicted kinetic parameters as DHT or t-AND concentration increased, the substrate inhibition kinetic profile of TAM glucuronidation became more hyperbolic (Figure 8). Various two-site models were tested to simultaneously fit the kinetic data. The derived kinetic parameters are presented in Table 2. Kinetic model in Figure 2C (Equation 9) adequately described the effect of DHT on TAM

glucuronidation and the fit of the data is presented in Figure 8A. For TAM glucuronidation kinetics in the presence of t-AND, two kinetic models (Figure 2D and Equation 10; Figure 2E and Equation 11) were applied to describe the kinetic data and similar goodness of fit was obtained. The fit of data to Equation 11 (Figure 2E) is illustrated in Figure 8B.

Discussion

In the present study, DHT and t-AND (more commonly known as epiandrosterone) were used as probe substrates to evaluate the potential existence of multiple aglycone substrate binding sites in UGT1A4. Glucuronidation of DHT and t-AND by HEK293-expressed UGT1A4 was evaluated in the presence of another UGT1A4 substrate, TAM or LTG. Unexpectedly, neither TAM nor LTG competitively inhibited DHT and t-AND glucuronidation. Noncompetitive inhibition was observed when LTG was used as the modifier, whereas concentration-dependent activation/ inhibition was observed with TAM as the modifier. These results, combined with kinetic modeling using various two-site models, suggest that multiple substrate binding sites exist in UGT1A4.

The glucuronidation kinetics of the four UGT1A4 substrates under investigation were carefully characterized. DHT and LTG exhibited hyperbolic kinetics, whereas t-AND and TAM displayed substrate inhibition kinetics. Although previous studies reported hyperbolic kinetics for TAM glucuronidation by UGT1A4 (Kaku et al., 2004; Sun et al., 2006), there are possible explanations for this discrepancy. In one report, a narrow TAM concentration range (1-6 μM, uncorrected for non-specific binding) was employed, potentially precluding the observation of substrate inhibition at higher TAM concentrations (Sun et al., 2006). In the second case, a one-hour incubation was conducted (Kaku et al., 2004), suggesting that linear incubation conditions may not have been

operational. Our preliminary studies to determine linearity with incubation time and protein concentration for TAM glucuronidation indicated that a low protein concentration and short incubation time were required to maintain steady state conditions.

In the present study, TAM and t-AND substrate inhibition were described with a two-site model, as depicted in Figure 2A (Equation 7). In both cases, the estimated b values were less than 1, indicating that the SES complex is less productive than the ES complex. Also, consistent with the more pronounced substrate inhibition of TAM glucuronidation, the estimated b value for TAM glucuronidation is smaller than the b value obtained for t-AND glucuronidation.

For UGT-catalyzed glucuronidation, substrate inhibition kinetics can also be explained by the aglycone substrate binding to the enzyme-UDP complex, resulting in a non-productive dead-end complex (Luukkanen et al., 2005). However, such mechanism where only one aglycone substrate binding site is incorporated inadequately explain the activation effect of TAM on DHT and t-AND glucuronidation. UDP, a product of catalysis, has been reported to be an inhibitor for UGT1A4 (IC_{50}=31μM) (Fujiwara et al., 2008). It is also possible that the observed substrate inhibition is due to the increased amount of UDP formation at high substrate concentrations. However, the calculated maximum UDP concentration was ~0.5 μM in our study. Thus, the inhibition of UGT1A4 by UDP should be negligible under the incubation conditions used herein.

A few cases of heteroactivation have been reported with UGTs (Williams et al., 2002; Mano et al., 2004; Pfeiffer et al., 2005; Uchaipichat et al., 2008; Hyland et al., 2009). Interestingly, in the present study TAM both activated and inhibited DHT glucuronidation in a concentration-dependent fashion. A two-site kinetic model (Figure 2B, Equation 8) which considers the kinetic properties of DHT and TAM adequately explained the effect of TAM on DHT glucuronidation. In this model, the overall effect of TAM is controlled by three enzyme-associated complexes (E-TAM, TAM-E-TAM, and TAM-E-DHT). Complexes E-TAM and TAM-E-TAM are not productive. The presence of these complexes results in less enzyme available for association with the substrate (DHT), producing an inhibition effect. However, the DHT-E-TAM complex is more productive than the DHT-E complex (c=8.36). The presence of the DHT-E-TAM complex leads to activation. At low TAM concentrations, the activation resulting from the presence of the DHT-E-TAM complex overcomes the inhibition effect, resulting in an overall activation effect. At high TAM concentrations, the TAM-E-TAM complex becomes the dominant form for TAM associating with the enzyme, resulting in an overall inhibition effect. Also interestingly, in contrast to most previous reports of enzyme heteroactivation, where the extent of heteroactivation decreases as the substrate concentration increases (Hutzler et al., 2001; Kenworthy et al., 2001; Uchaipichat et al., 2008), DHT glucuronidation is increasingly heteroactivated by TAM as the substrate (DHT) concentration was increased. This discrepancy is likely due to different mechanisms of heteroactivation. In previous cases,

heteroactivation was largely due to the positive cooperative binding of substrates and modifiers to the enzyme (Hutzler et al., 2001; Kenworthy et al., 2001; Uchaipichat et al., 2008). However, in the present study, the increased glucuronidation appeared to be due to the presence of a more productive modifier-E-substrate complex (DHT-E-TAM) (c=8.36). The percentage of the DHT-E-TAM complex among all enzyme complexes is greater at high substrate concentrations than at low substrate concentrations and therefore more activation was observed at high substrate concentrations.

Assuming the same binding scenario as in Figure 2B (Equation 8), kinetic model in Figure 2C (Equation 9) adequately explained the effect of DHT on TAM glucuronidation. But in this case, the predicted c value is less than 1, indicating the DHT-E-TAM complex is less productive than the E-TAM complex, consistent with the observed inhibition effect of DHT on TAM glucuronidation. In addition, in this model TAM substrate inhibition kinetics would be eliminated as DHT-E-TAM becomes the dominant productive complex, also consistent with our observation that the substrate inhibition kinetic profile of TAM glucuronidation became more hyperbolic as DHT concentration was increased.

Albeit modest activation, TAM exhibits the same effect on t-AND glucuronidation as on DHT glucuronidation: concentration-dependent activation/inhibition and greater activation at higher substrate concentrations. However, the kinetic model in Figure 2B (Equation 9) may not adequately explain the interactions of TAM on t-AND glucuronidation due to the substrate inhibition kinetics of t-AND (two t-

AND binding sites). Kinetic models in which t-AND and TAM both have two binding sites on UGT1A4 may be applicable. Kinetic modeling with more data points than obtained in Figure 4B is needed to adequately characterize the effect of TAM on t-AND glucuronidation.

Kinetic studies to characterize the effect t-AND on TAM glucuronidation was carefully conducted. Two kinetic models (Figure 2D and Equation 10; Figure 2E and Equation 11) in which the two binding sites of t-AND overlap with the two binding sites of TAM adequately explained the kinetic data. Again the predicted c values (less than 1) are consistent with the inhibition effect of t-AND on TAM glucuronidation and TAM substrate inhibition kinetics being eliminated as the less productive t-AND-E-TAM complex becomes the dominant productive complex in the models is consistent with our observation.

The unexpected heteroactivation on DHT and t-AND glucuronidation by TAM led us to investigate the effect of TAM on UGT1A4 activity with a different type of UGT1A4 substrate: LTG (an aromatic amine substrate of UGT1A4). In contrast to the concentration-dependent activation/inhibition on DHT and t-AND glucuronidation, LTG N-glucuronidation was competitively inhibited by TAM, suggesting that the heteroactivation of UGT1A4-catalyzed glucuronidation by TAM is substrate-dependent.

LTG was also evaluated as a modifier on DHT and t-AND glucuronidation. LTG inhibited both t-AND and DHT glucuronidation, but interestingly the one-site

noncompetitive inhibition model (Equation 5) better described the kinetic data than the one-site competitive inhibition model (Equation 4). The observed noncompetitive inhibition of DHT glucuronidation by LTG suggests that these two UGT1A4 substrates have distinct binding sites within the active site of UGT1A4, assuming each has only one binding site.

The present study provides compelling evidence for the existence of at least two aglycone binding sites in UGT1A4. Though models can be developed to describe the kinetic data, additional biophysical/ biochemical studies are needed to delineate the specific binding region(s) of each molecule in UGT1A4. Additional kinetic studies with a wider range of UGT1A4 substrates are also needed to evaluate the range of substrates for which atypical kinetics are operable. UGT1A4 has been reported to form homodimers (Operana and Tukey, 2007), which may also play a role in these atypical kinetic phenomena. It is yet to be determined whether the two aglycone binding sites exist in different monomers or whether each monomer has two separate aglycone binding sites.

In vitro- in vivo extrapolations for UGT-catalyzed metabolism have proven problematic for a number of reasons, including inability to estimate in vivo UGT enzyme amounts, lack of isoform-specific probe substrates and inhibitors, overlapping substrate specificities (Miners et al., 2004; Miners et al., 2006) and “albumin effect”(Rowland et al., 2008). Accumulating evidence from the current study and others referenced above suggests that atypical kinetics involving this enzyme family may also contribute to the difficulty in making in vitro-in vivo

correlations. Atypical kinetic profiles, such as the substrate inhibition observed in the present study, complicate the estimation of intrinsic clearance. Additionally, the presence of multiple aglycone binding sites and the substrate-dependent heteroactivation as observed in the present study, complicate the prediction of drug interactions. In summary, the present study reinforces the need for careful characterization of UGT1A4 kinetics and highlights the caveats of making in vitro-in vivo correlations with this important metabolizing enzyme. For the purpose of screening for UGT1A4 inhibitors, the present study suggests the potential need to employ multiple probe substrates.

Acknowledgements

The authors wish to thank Dr. Philip Lazarus at Pennsylvania State University for providing transfected HEK-293 cells that express UGT1A4. Synthesis of tamoxifen N-glucuronide was done with the help of Dr. Courtney Aldrich, Center for Drug Design, University of Minnesota. Morphine-3-glucuronide was a gift from Dr. Cheryl Zimmerman, University of Minnesota.

References

Chouinard S, Tessier M, Vernouillet G, Gauthier S, Labrie F, Barbier O and Belanger A (2006) Inactivation of the pure antiestrogen fulvestrant and other synthetic estrogen molecules by UDP-glucuronosyltransferase 1A enzymes expressed in breast tissue. *Mol Pharmacol* **69:**908-920.

Collom SL, Laddusaw RM, Burch AM, Kuzmic P, Perry MD, Jr. and Miller GP (2008) CYP2E1 substrate inhibition. Mechanistic interpretation through an effector site for monocyclic compounds. *J Biol Chem* **283:**3487-3496.

Fisher MB, Campanale K, Ackermann BL, VandenBranden M and Wrighton SA (2000) In vitro glucuronidation using human liver microsomes and the pore-forming peptide alamethicin. *Drug Metab Dispos* **28:**560-566.

Fujiwara R, Nakajima M, Yamanaka H, Katoh M and Yokoi T (2008) Product inhibition of UDP-glucuronosyltransferase (UGT) enzymes by UDP obfuscates the inhibitory effects of UGT substrates. *Drug Metab Dispos* **36:**361-367.

Galetin A, Clarke SE and Houston JB (2002) Quinidine and haloperidol as modifiers of CYP3A4 activity: multisite kinetic model approach. *Drug Metab Dispos* **30:**1512-1522.

Green MD and Tephly TR (1996) Glucuronidation of amines and hydroxylated xenobiotics and endobiotics catalyzed by expressed human UGT1.4 protein. *Drug Metab Dispos* **24:**356-363.

Hallifax D and Houston JB (2006) Binding of drugs to hepatic microsomes: comment and assessment of current prediction methodology with recommendation for improvement. *Drug Metab Dispos* **34:**724-726; author reply 727.

Hashizume T, Xu Y, Mohutsky MA, Alberts J, Hadden C, Kalhorn TF, Isoherranen N, Shuhart MC and Thummel KE (2008) Identification of human UDP-glucuronosyltransferases catalyzing hepatic 1alpha,25-dihydroxyvitamin D3 conjugation. *Biochem Pharmacol* **75:**1240-1250.

Houston JB and Kenworthy KE (2000) In vitro-in vivo scaling of CYP kinetic data not consistent with the classical Michaelis-Menten model. *Drug Metab Dispos* **28:**246-254.

Hutzler JM, Hauer MJ and Tracy TS (2001) Dapsone activation of CYP2C9-mediated metabolism: evidence for activation of multiple substrates and a two-site model. *Drug Metab Dispos* **29:**1029-1034.

Hyland R, Osborne T, Payne A, Kempshall S, Logan YR, Ezzeddine K and Jones B (2009) In vitro and in vivo glucuronidation of midazolam in humans. *Br J Clin Pharmacol* **67:**445-454.

Iwuchukwu OF and Nagar S (2008) Resveratrol (trans-resveratrol, 3,5,4'-trihydroxy-trans-stilbene) glucuronidation exhibits atypical enzyme kinetics in various protein sources. *Drug Metab Dispos* **36:**322-330.

Kaku T, Ogura K, Nishiyama T, Ohnuma T, Muro K and Hiratsuka A (2004) Quaternary ammonium-linked glucuronidation of tamoxifen by human liver microsomes and UDP-glucuronosyltransferase 1A4. *Biochem Pharmacol* **67:**2093-2102.

Kenworthy KE, Clarke SE, Andrews J and Houston JB (2001) Multisite kinetic models for CYP3A4: simultaneous activation and inhibition of diazepam and testosterone metabolism. *Drug Metab Dispos* **29:**1644-1651.

Kiang TK, Ensom MH and Chang TK (2005) UDP-glucuronosyltransferases and clinical drug-drug interactions. *Pharmacol Ther* **106:**97-132.

Korzekwa KR, Krishnamachary N, Shou M, Ogai A, Parise RA, Rettie AE, Gonzalez FJ and Tracy TS (1998) Evaluation of atypical cytochrome P450 kinetics with two-substrate models: evidence that multiple substrates can simultaneously bind to cytochrome P450 active sites. *Biochemistry* **37:**4137-4147.

Lin Y, Lu P, Tang C, Mei Q, Sandig G, Rodrigues AD, Rushmore TH and Shou M (2001) Substrate inhibition kinetics for cytochrome P450-catalyzed reactions. *Drug Metab Dispos* **29:**368-374.

Luukkanen L, Taskinen J, Kurkela M, Kostiainen R, Hirvonen J and Finel M (2005) Kinetic characterization of the 1A subfamily of recombinant human UDP-glucuronosyltransferases. *Drug Metab Dispos* **33:**1017-1026.

Mackenzie PI, Rogers A, Treloar J, Jorgensen BR, Miners JO and Meech R (2008) Identification of UDP glycosyltransferase 3A1 as a UDP N-acetylglucosaminyltransferase. *J Biol Chem* **283:**36205-36210.

Mano Y, Usui T and Kamimura H (2004) Effects of beta-estradiol and propofol on the 4-methylumbelliferone glucuronidation in recombinant human UGT isozymes 1A1, 1A8 and 1A9. *Biopharm Drug Dispos* **25:**339-344.

Miley MJ, Zielinska AK, Keenan JE, Bratton SM, Radominska-Pandya A and Redinbo MR (2007) Crystal structure of the cofactor-binding domain of the human phase II drug-metabolism enzyme UDP-glucuronosyltransferase 2B7. *J Mol Biol* **369:**498-511.

Miners JO, Knights KM, Houston JB and Mackenzie PI (2006) In vitro-in vivo correlation for drugs and other compounds eliminated by glucuronidation in humans: pitfalls and promises. *Biochem Pharmacol* **71:**1531-1539.

Miners JO, Smith PA, Sorich MJ, McKinnon RA and Mackenzie PI (2004) Predicting human drug glucuronidation parameters: application of in vitro and in silico modeling approaches. *Annu Rev Pharmacol Toxicol* **44:**1-25.

Ohno S, Kawana K and Nakajin S (2008) Contribution of UDP-glucuronosyltransferase 1A1 and 1A8 to morphine-6-glucuronidation and its kinetic properties. *Drug Metab Dispos* **36:**688-694.

Operana TN and Tukey RH (2007) Oligomerization of the UDP-glucuronosyltransferase 1A proteins: homo- and heterodimerization analysis by fluorescence resonance energy transfer and co-immunoprecipitation. *J Biol Chem* **282:**4821-4829.

Pfeiffer E, Treiling CR, Hoehle SI and Metzler M (2005) Isoflavones modulate the glucuronidation of estradiol in human liver microsomes. *Carcinogenesis* **26:**2172-2178.

Radominska-Pandya A, Czernik PJ, Little JM, Battaglia E and Mackenzie PI (1999) Structural and functional studies of UDP-glucuronosyltransferases. *Drug Metab Rev* **31:**817-899.

Rios GR and Tephly TR (2002) Inhibition and active sites of UDP-glucuronosyltransferases 2B7 and 1A1. *Drug Metab Dispos* **30:**1364-1367.

Rowland A, Elliot DJ, Knights KM, Mackenzie PI and Miners JO (2008) The "albumin effect" and in vitro-in vivo extrapolation: sequestration of long-chain unsaturated fatty acids enhances phenytoin hydroxylation by human liver microsomal and recombinant cytochrome P450 2C9. *Drug Metab Dispos* **36:**870-877.

Rowland A, Elliot DJ, Williams JA, Mackenzie PI, Dickinson RG and Miners JO (2006) In vitro characterization of lamotrigine N2-glucuronidation and the lamotrigine-valproic acid interaction. *Drug Metab Dispos* **34:**1055-1062.

Schrag ML and Wienkers LC (2001) Triazolam substrate inhibition: evidence of competition for heme-bound reactive oxygen within the CYP3A4 active site. *Adv Exp Med Biol* **500:**347-350.

Segel I (1993) *Enzyme Kinetics: Behavior and Analysis of Rapid Equilibrium and Steady-State Enzyme Systems*. Wiley Classics Library, Ney Jersey.

Shou M, Dai R, Cui D, Korzekwa KR, Baillie TA and Rushmore TH (2001) A kinetic model for the metabolic interaction of two substrates at the active site of cytochrome P450 3A4. *J Biol Chem* **276:**2256-2262.

Shou M, Grogan J, Mancewicz JA, Krausz KW, Gonzalez FJ, Gelboin HV and Korzekwa KR (1994) Activation of CYP3A4: evidence for the simultaneous binding of two substrates in a cytochrome P450 active site. *Biochemistry* **33:**6450-6455.

Sun D, Chen G, Dellinger RW, Duncan K, Fang JL and Lazarus P (2006) Characterization of tamoxifen and 4-hydroxytamoxifen glucuronidation by human UGT1A4 variants. *Breast Cancer Res* **8:**R50.

Tukey RH and Strassburg CP (2000) Human UDP-glucuronosyltransferases: metabolism, expression, and disease. *Annu Rev Pharmacol Toxicol* **40:**581-616.

Uchaipichat V, Galetin A, Houston JB, Mackenzie PI, Williams JA and Miners JO (2008) Kinetic modeling of the interactions between 4-methylumbelliferone, 1-naphthol, and zidovudine glucuronidation by udp-glucuronosyltransferase 2B7 (UGT2B7) provides evidence for multiple substrate binding and effector sites. *Mol Pharmacol* **74:**1152-1162.

Uchaipichat V, Mackenzie PI, Guo XH, Gardner-Stephen D, Galetin A, Houston JB and Miners JO (2004) Human udp-glucuronosyltransferases: isoform selectivity and kinetics of 4-methylumbelliferone and 1-naphthol glucuronidation, effects of organic solvents, and inhibition by diclofenac and probenecid. *Drug Metab Dispos* **32:**413-423.

Williams JA, Ring BJ, Cantrell VE, Campanale K, Jones DR, Hall SD and Wrighton SA (2002) Differential modulation of UDP-glucuronosyltransferase 1A1 (UGT1A1)-catalyzed estradiol-3-glucuronidation by the addition of UGT1A1 substrates and other

compounds to human liver microsomes. *Drug Metab Dispos* **30:**1266-1273.

Footnotes

Financial support for this work was in the form of an investigator-initiated grant from Bristol-Myers Squibb to R.P. R. and by the National Institutes of Health [Grants GM063215] to T.S.T. A grant from Shimadzu Corp. was awarded for the purchase of Shimadzu LCMS-2010A instrument used in this study.

Reprint requests: *Rory P. Remmel, Ph.D, Department of Medicinal Chemistry, University of Minnesota, 8-101 WDH, 308 Harvard Street, Minneapolis, MN 55455. E-mail:* remme001@umn.edu

Legends for Figures

Figure 1. Structures of DHT, t-AND, TAM and LTG,

The glucuronidation sites of the compounds are illustrated with arrows.

Figure 2. Two-site kinetic models. (new figure)

A: a kinetic model for substrate inhibition kinetics (Equation 7); B: a kinetic model to explain the effect of TAM on DHT glucuronidation (Equation 8); C: a kinetic model to explain the effect of DHT on TAM glucuronidation (Equation 9); D and E: kinetic models to explain the effect of t-AND on TAM glucuronidation (Equation 10 and 11). k_p is the effective catalytic constant. K_s, K_{DHT}, $K_{t\text{-}AND}$, K_{TAM} are binding affinity constants. Constant b and c reflect change in k_p and constant d reflects changes in binding affinity.

Figure 3. Kinetic plots (Rate versus [S]) for DHT (A) and t-AND (B) glucuronidation by recombinant UGT1A4.

The bars indicate the range of triplicate measurements. The embedded figures are Eadie-Hofstee plots for the same data. The Michaelis-Menten equation (Equation 2) was fit to the data for DHT glucuronidation. The uncompetitive substrate inhibition equation (Equation 3) was fit to the data for t-AND glucuronidation.

Figure 4. Rate percentage of control versus [S] plots.

A: for the effect of TAM on DHT glucuronidation; B: for the effect of TAM on t-AND glucuronidation; C: for the effect of LTG on DHT glucuronidation; D: for the effect of LTG on t-AND glucuronidation; E: for the effect of TAM on LTG

glucuronidation. Data points are means of duplicate measurements. Coefficients of variation are all within 10%. Symbols in Figure A represent DHT concentrations: 2.5 (●), 5 (○), 10 (▼), 20 (Δ), 40 (■), 80 (□), 100 (♦). Symbols in Figure B, C and D represent DHT and t-AND concentrations: 10 (●), 20(○), 40 (▼) μM. Symbols in Figure E represent LTG concentrations: 0.75 (●), 1.5(○), 3.0(▼) mM. TAM concentration in the plots was corrected for non-specific protein binding. Controls refer to incubations in which the concentration of the modifier was zero.

Figure 5. Kinetic modeling for the effect of TAM on DHT glucuronidation. The surface plot was predicted with Equation 8 (Figure 2B) and the TAM concentration in the plot was corrected for non-specific protein binding.

Figure 6. Kinetic plots (Rate versus [S]) for TAM glucuronidation by recombinant UGT1A4.

The bars indicate the range of triplicate measurements. The embedded figures are Eadie-Hofstee plots for the same data. A two-site model (Figure 2A and Equation 7) was fit to the data.

Figure 7. Dixon plots.

A: for inhibition of DHT glucuronidation by LTG; B: for inhibition of t-AND glucuronidation by LTG; C: for inhibition of LTG glucuronidation by TAM. The bars indicate the range of duplicate measurements. A one-site non-competitive inhibition model (Equation 5) was fit to the data in Figure A and B. Symbols represent DHT and t-AND concentrations: 10 (●), 20(○), 40 (▼) μM. A one-site

competitive inhibition model (Equation 4) was fit to the data in Figure C. Symbols represent LTG concentrations: 0.75 (●), 1.5(○), 3.0(▼) mM. The TAM concentration in Figure C was corrected for non-specific protein binding.

Figure 8. Kinetic modeling for effect of DHT (A) and t-AND (B) on TAM glucuronidation.

The surface plot in Figure A is a predicted result with Equation 9 (Figure 2C) and the surface plot in Figure B is a predicted result with Equation 11 (Figure 2E). The TAM concentration was corrected for non-specific protein binding.

DMD Fast Forward. Published on December 9, 2009 as DOI: 10.1124/dmd.109.028712
This article has not been copyedited and formatted. The final version may differ from this version.

Table 1. Kinetic parameters for the glucuronidation of DHT, t-AND, TAM and LTG by recombinant UGT1A4. [a] Standard errors; [b] Not applicable

Substrate	K_m *(μM)*	V_{max} *(pmol/min/mg of protein)*	K_{si} *(μM)*	*Kinetics Model*	R^2
DHT	19.6 (2.2)[a]	17.1 (0.44)[a]	NA[b]	Michaelis-Menten (Equation 2)	0.9404
t-AND	23.6 (3.1)[a]	114 (7.2)[a]	514 (133)[a]	Uncompetitive substrate inhibition (Equation 3)	0.9755
TAM	0.90 (0.14)[a]	447 (37)[a]	4.6 (0.71)[a]	Uncompetitive substrate inhibition (Equation 3)	0.9639
LTG	1564 (126)[a]	1064 (33)[a]	NA[b]	Michaelis-Menten (Equation 2)	0.9926

Table 2. Kinetic parameters obtained by fitting various two-site models to kinetic data.

[a] Standard errors; [b] Not applicable, K_{sub} and K_{mod} refer to the binding affinity of the substrate and modifier to the enzyme.

Substrate	*Modifier*	*V_{max}* *(pmol/min/mg of protein)*	*K_{sub}* *(μM)*	*K_{mod}* *(μM)*	*b*	*c*	*d*	Kinetic model	*R^2*
t-AND	without modifier	127 (19)[a]	33 (6.0)[a]	N.A.	0.56 (0.12)[a]	N.A.	N.A.	Equation 7	0.9695
TAM	without modifier	625 (22)[a]	1.4 (0.12)[a]	NA[b]	0.12 (0.02)[a]	N.A.	N.A.	Equation 7	0.9712
DHT	TAM	9.8 (0.45)[a]	18 (2.2)[a]	0.35 (0.02)[a]	N.A	8.4 (3.0)[a]	4.4 (2.1)[a]	Equation 8	0.9911
TAM	DHT	562 (43)[a]	1.8 (0.24)[a]	58 (17)[a]	0.10 (0.04)[a]	0.52 (0.20)[a]	2.9 (1.9)[a]	Equation 9	0.9743
TAM	t-AND	761 (51)[a]	1.3 (0.11)[a]	106 (21)[a]	0.18 (0.03)[a]	0.28 (0.12)[a]	1.2 (0.33)[a]	Equation 10	0.9795
TAM	t-AND	761 (51)[a]	1.3 (0.11)[a]	106 (21)[a]	0.18 (0.03)[a]	0.14 (0.06)[a]	0.57 (0.17)[a]	Equation 11	0.9795

DMD Fast Forward. Published on December 9, 2009 as DOI: 10.1124/dmd.109.028712
This article has not been copyedited and formatted. The final version may differ from this version.

Table 3. Kinetic parameters for DHT glucuronidation in the presence or absence of TAM. The Michaelis-Menten equation (Equation 2) was used to fit individual kinetic data set. [a] Standard errors; CL_{int} equates to V_{max}/K_m; The TAM concentration was corrected for non-specific binding

[TAM] (μM)	K_m (μM)	V_{max} (pmol/min/mg of protein)	CL_{int} (μl/min/mg of protein)
0	17 (1.6)[a]	9.5 (0.3)[a]	0.55
0.11	22 (2.5)[a]	15 (0.60)[a]	0.67
0.23	29 (3.3)[a]	18 (0.79)[a]	0.63
0.45	61 (4.9)[a]	27 (1.1)[a]	0.45
0.90	185 (32)[a]	47(5.7)[a]	0.25
1.80	227 (89)[a]	47 (14)[a]	0.20

Figure 1

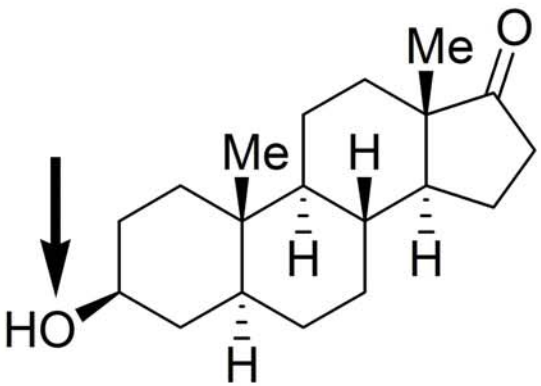

Trans-androsterone

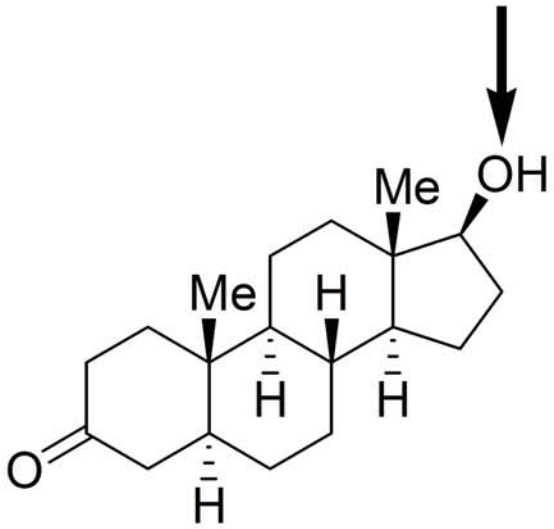

Dihydrotestosterone

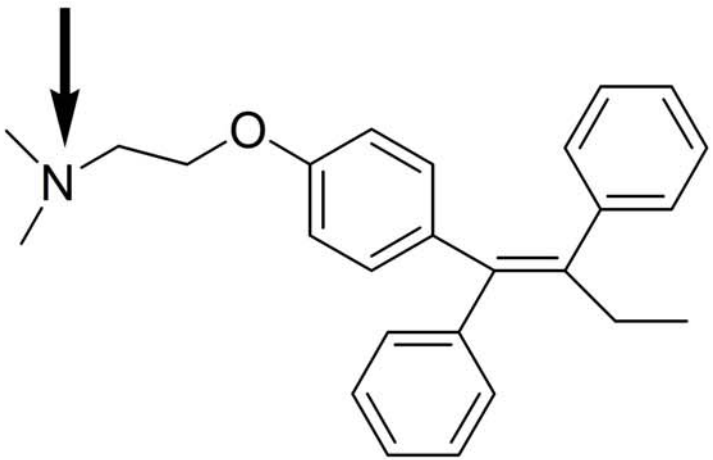

Tamoxifen

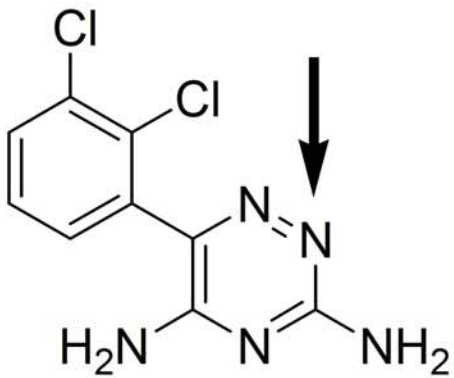

Lamotrigine

Figure 2

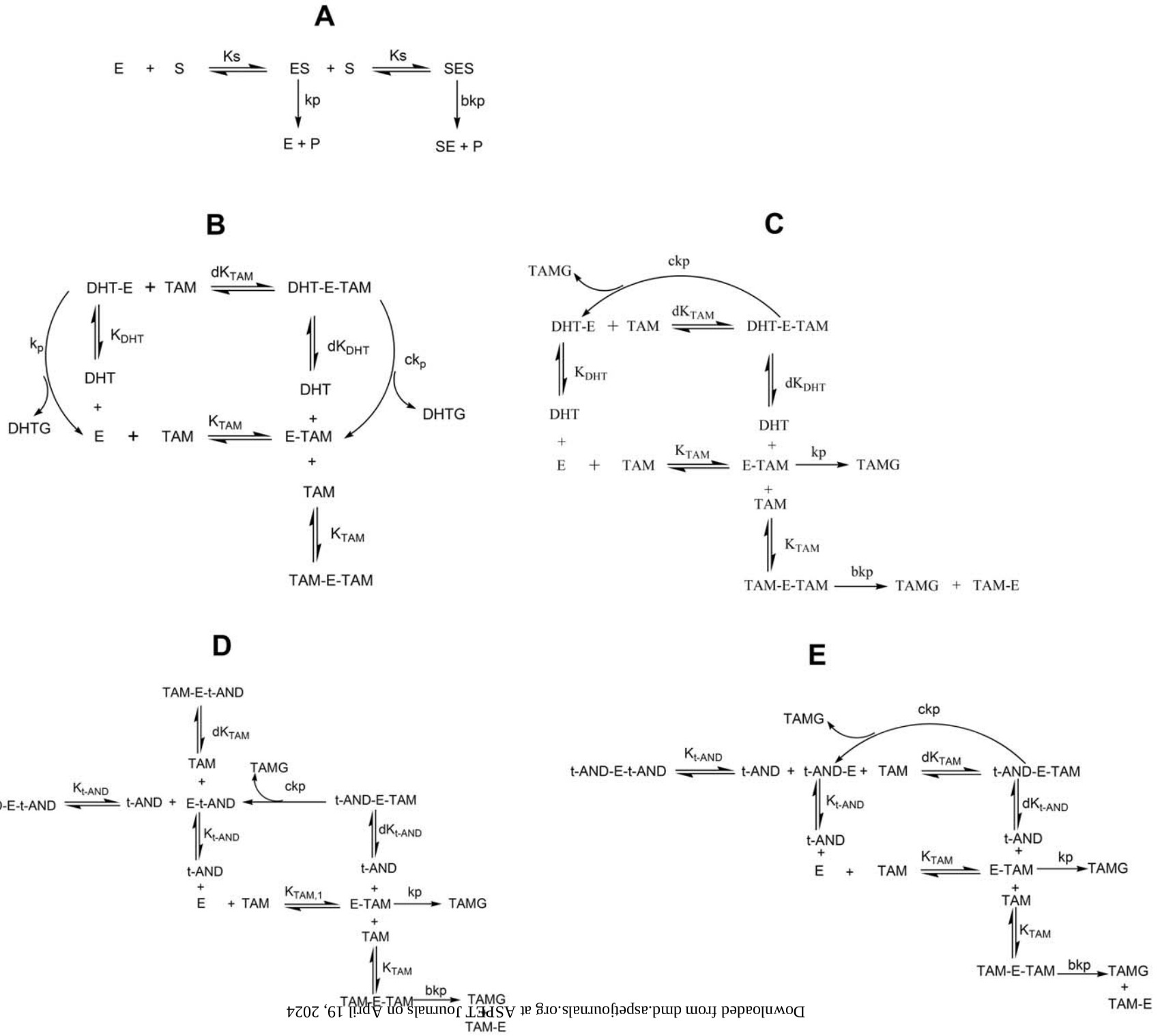

DMD Fast Forward. Published on December 9, 2009 as DOI: 10.1124/dmd.109.028712
This article has not been copyedited and formatted. The final version may differ from this version.

Figure 3

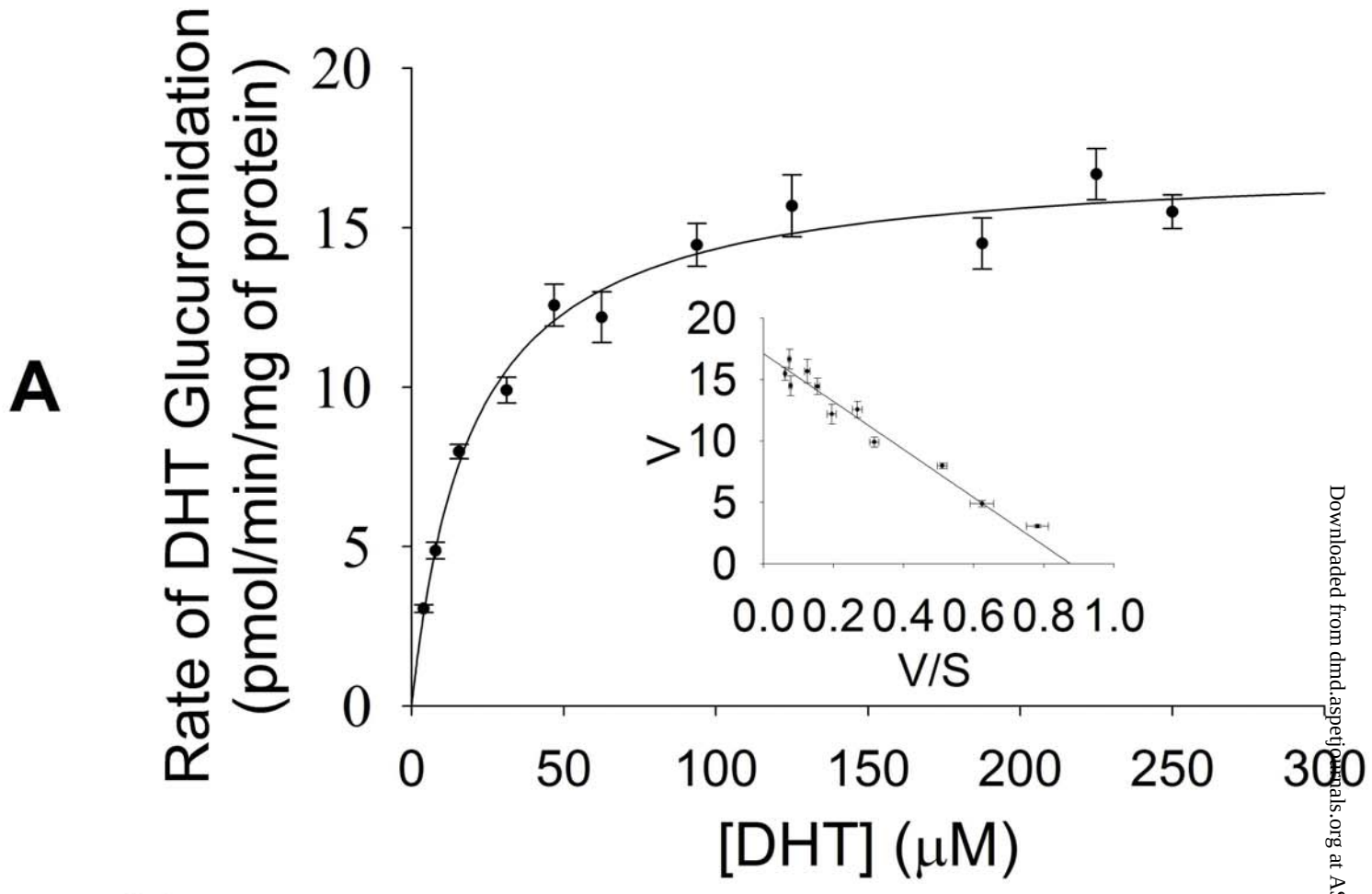

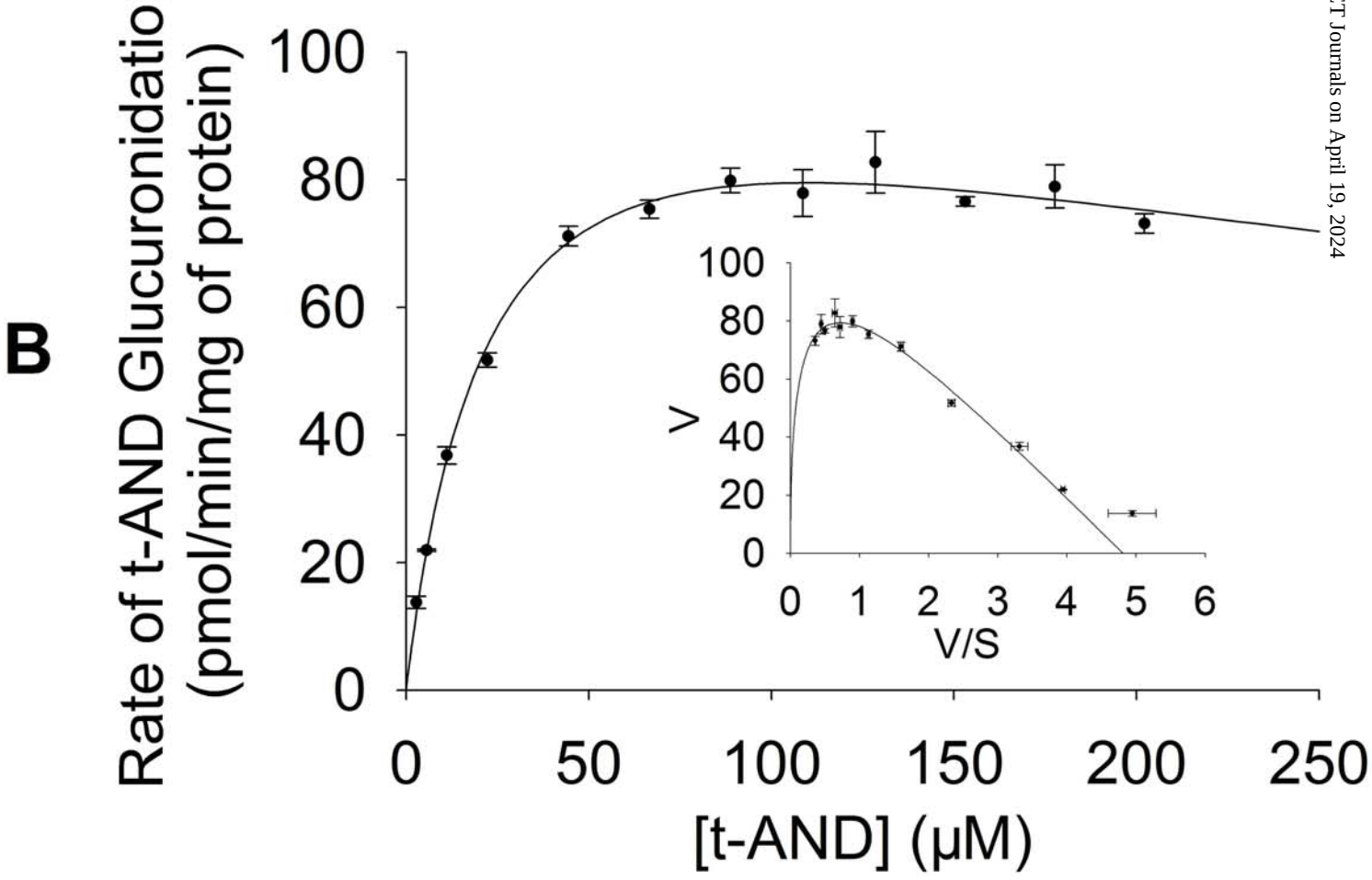

DMD Fast Forward. Published on December 9, 2009 as DOI: 10.1124/dmd.109.028712
This article has not been copyedited and formatted. The final version may differ from this version.

Figure 4

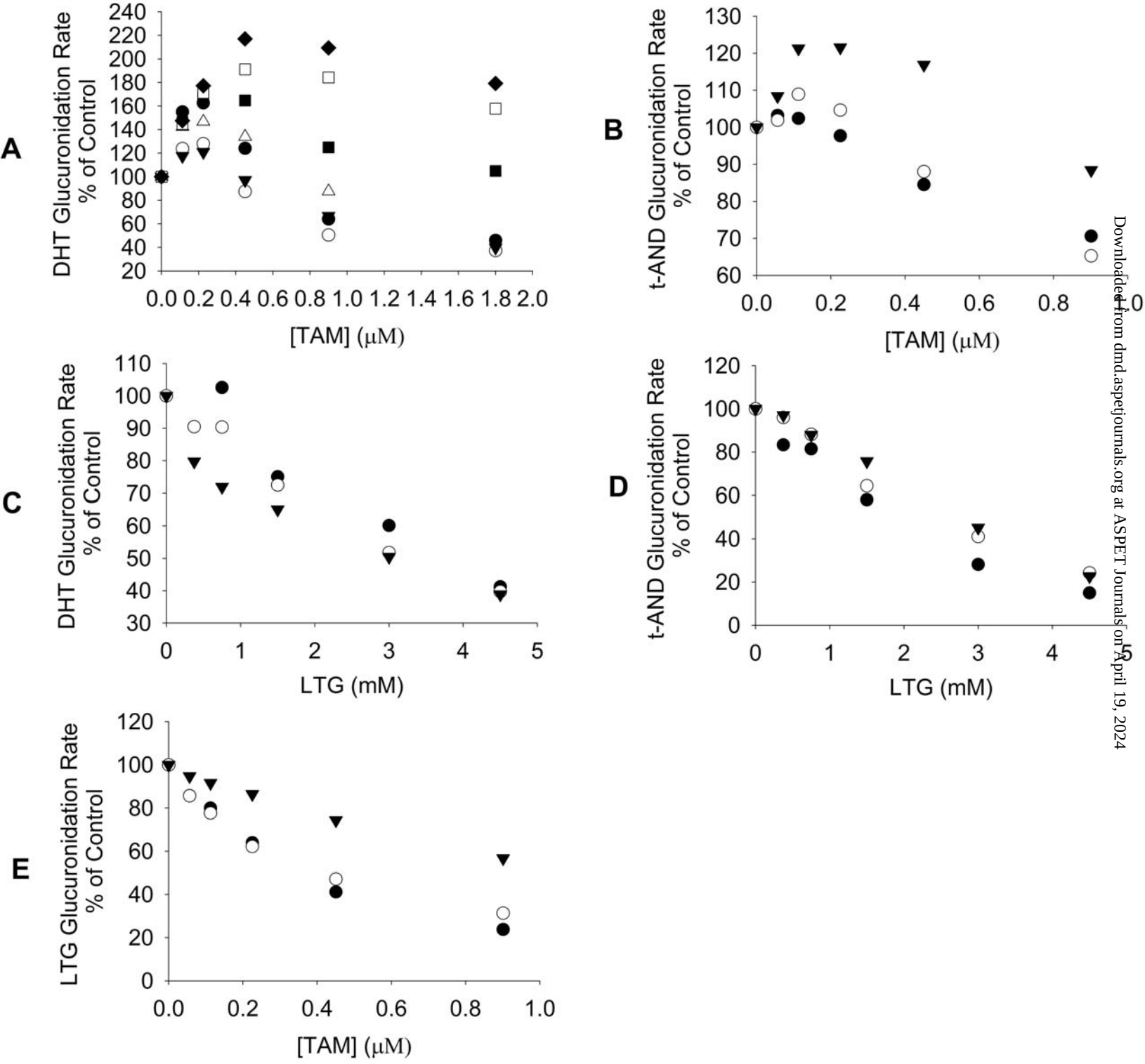

DMD Fast Forward. Published on December 9, 2009 as DOI: 10.1124/dmd.109.028712
This article has not been copyedited and formatted. The final version may differ from this version.

Figure 5

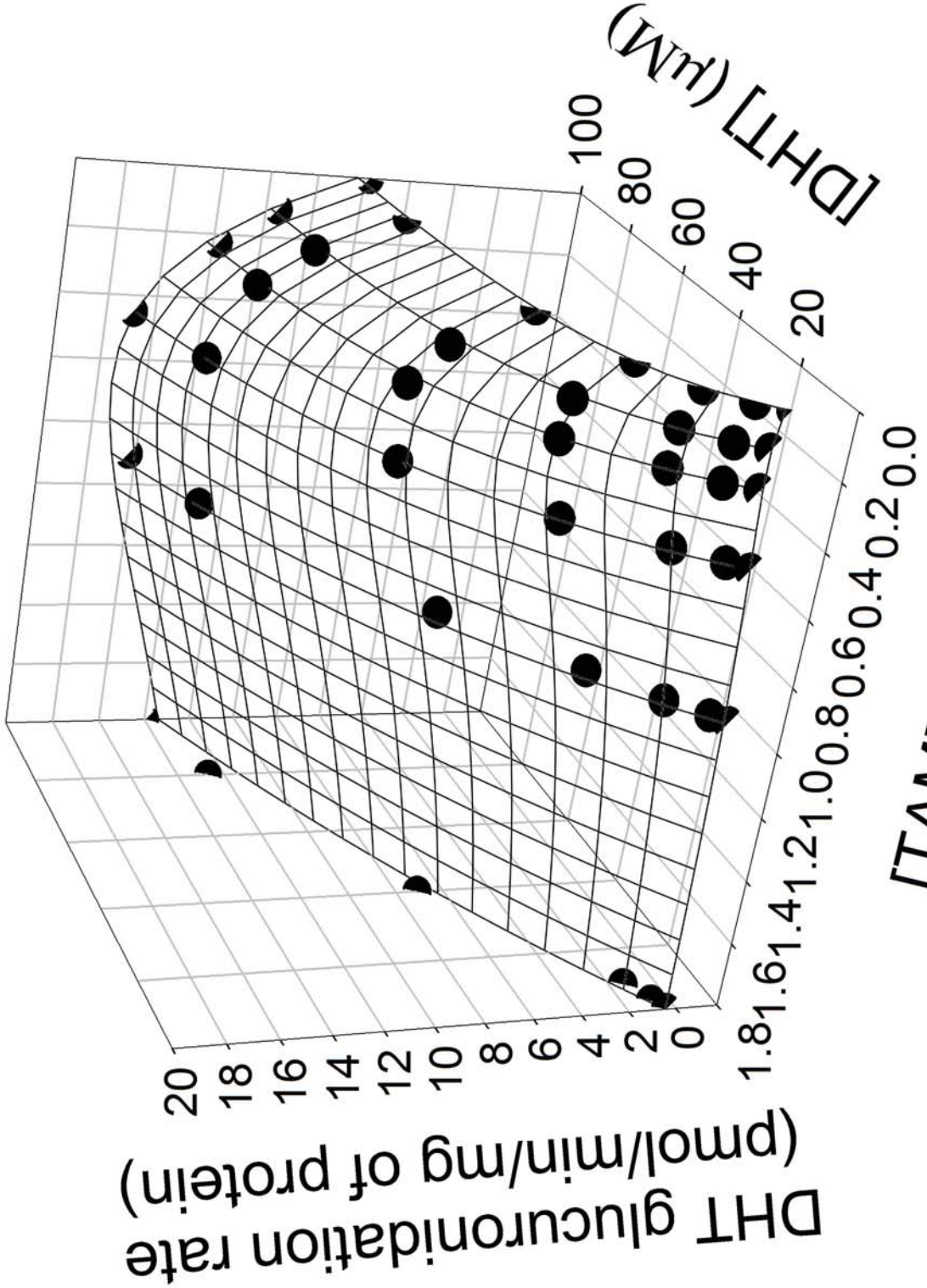

DMD Fast Forward. Published on December 9, 2009 as DOI: 10.1124/dmd.109.028712
This article has not been copyedited and formatted. The final version may differ from this version.

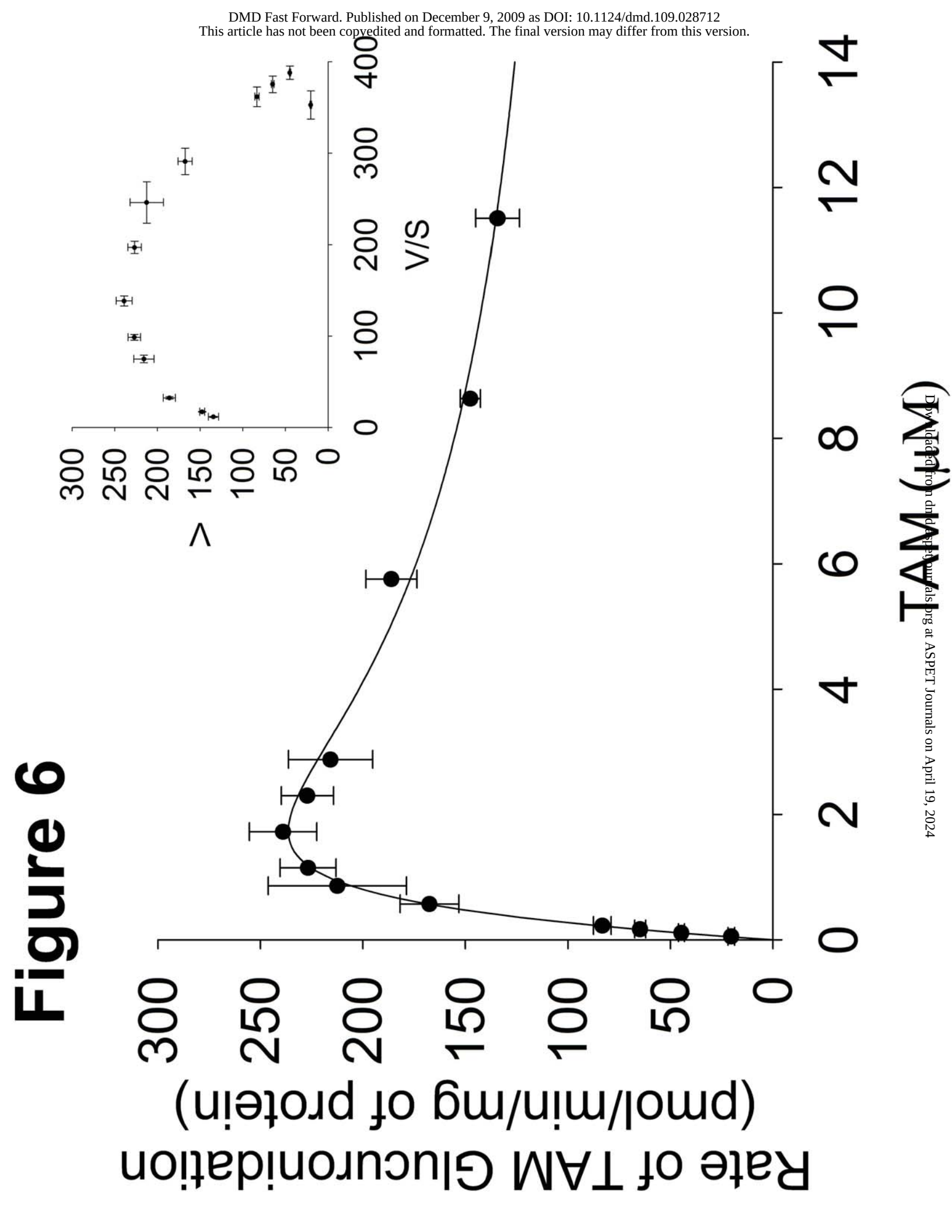

DMD Fast Forward. Published on December 9, 2009 as DOI: 10.1124/dmd.109.028712
This article has not been copyedited and formatted. The final version may differ from this version.

Figure 7

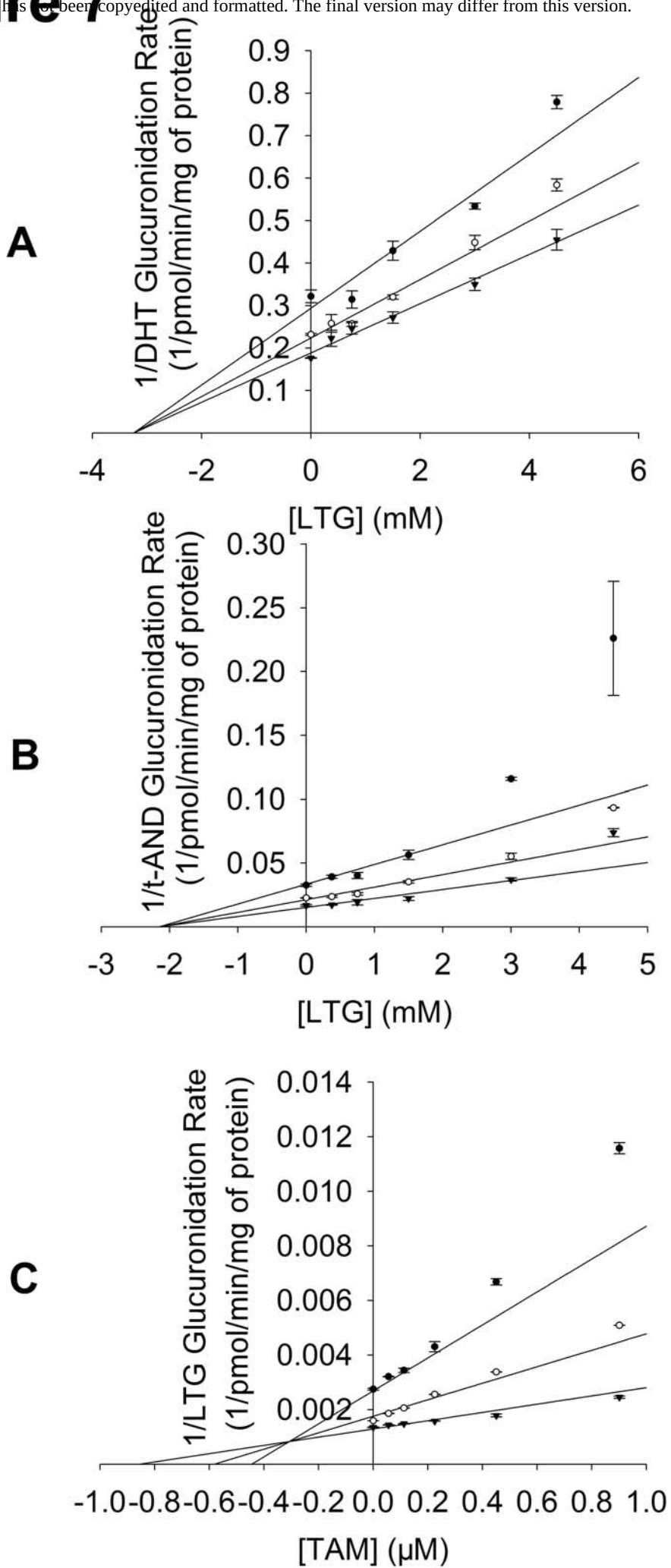

DMD Fast Forward. Published on December 9, 2009 as DOI: 10.1124/dmd.109.028712

Figure 8